Luo and Liu *EURASIP Journal on Wireless Communications and Networking* (2017) 2017:123
DOI 10.1186/s13638-017-0911-6

EURASIP Journal on Wireless Communications and Networking

RESEARCH Open Access

# Serial distributed detection for wireless sensor networks with sensor failure

Junhai Luo* and Zuoting Liu

**Abstract**

We study serial distributed detection and fusion over noisy channels in wireless sensor networks (WSNs) with bathtub-shaped failure (BSF) rate of the sensors in this paper. In the previous work, we applied BSF rate to parallel topology and derived the Extension Log-likelihood Ration Test (ELRT) rule. Although ELRT is superior to traditional fusion rule without considering failed sensors, the detection performance decreases noticeably in the presence of a large number of failed sensors. In this paper, we construct a serial topology based on the target radiation energy attenuation model, apply BSF rate to serial topology, and derive the corresponding fusion rule. Unlike the parallel fusion, where the local sensors send their decisions to the Global Fusion Center (GFC) in the region of interest (ROI) directly, sensors in the serial topology transmit local decisions through multi-hop, short-range communications. At the same time, we extend ELRT to noisy channels. Finally, simulation results prove the effectiveness of the proposed fusion rules.

**Keywords:** Serial distributed detection, bathtub-shaped failure rate, failed sensors

## 1 Introduction

WSNs have attracted many researchers in various disciplines due to their flexibility, robustness, mobility, and cost-effectiveness. A major application of WSNs is target detection. WSN typically consists of a vast number of small, inexpensive, and low-powered sensors, which are deployed in the ROI to obtain and preprocess the received observation. The GFC is making a final decision about whether the target is present or not. There are two popular detection methods: centralized detection and distributed detection. In the centralized detection, the local sensor sends the received observation to the GFC directly without any processing. In the distributed detection, each sensor quantifies its observation into a local decision ("0" or "1") and sends it to the GFC. Although centralized detection achieves the highest performance, it is at the cost of more bandwidth and communication energy to obtain real-time results. Thus, the distributed detection is often preferable in these situations.

Distributed target detection has been extensively studied in many kinds of literature. In [1, 2], each sensor made a local decision by conducting likelihood ratio test and sent the local decision to the GFC to perform global log-likelihood ratio test, and then the GFC made a final decision. In [3], a uniformly most powerful (UMP) detector based on likelihood ratio test was developed, and an elegant test for target presence or absence was also derived. Typically, the performance of local sensors is hard to calculate. Therefore, in [4], a suboptimal fusion rule requiring less prior information was proposed, which we refer to as the counting rule (CR). CR employed the total number of decisions transmitted from local sensors for hypothesis testing at the GFC. In [5], CR was extended to the case where the total number of sensors was uncertain. Authors in [6–9] took into account imperfect communication channels between the sensors and the GFC, such as additive white Gaussian noise (AWGN) channels and fading channels. In [6], noisy communication links were considered and a Bayesian framework for distributed detection was presented, where noisy links were modeled as binary symmetric channels (BSC). In [7], distributed detection fusion in hierarchical WSNs was investigated in the presence of fading and noise, two fusion rules were derived accordingly, one utilized the complete fading channel state information (CSI), the other utilized the channel envelope statistics (CS). For resource-constrained sensor networks, a fusion rule using CSI was more preferable. Typically, local sensors communicated

*Correspondence: junhai_luo@uestc.edu.cn
School of Electronic Engineering, University of Electronic Science and Technology of China, No. 2006, Xiyuan Ave, West Hi-Tech Zone, 611731 Chengdu, China

with the GFC directly. In [10], authors considered the case where local decisions need to be relayed through the multi-hop transmission to reach the GFC and also took fading into account. In [11], based on various decisions from local sensors, a decision rule was derived in the case of unknown probability distributions. In [12, 13], decision fusion rules with unknown detection probability were investigated. Clustering-based decision fusion algorithms and fusion rules for distributed target detection in WSNs were studied in [14–16].

The structure of the WSNs can be classified into three categories: parallel topology, serial topology, and tree topology. Most researchers focus on parallel distributed detection. However, sensors are usually powered by a battery, so the energy and the communication range are limited. When sensors are far away from the GFC, the power consumption increases dramatically and the lifetime of the WSN has shortened accordingly. In [17, 18], serial distributed detection was investigated, where local decisions are transmitted to the GFC through short-range and multi-hop communication. The channel between two adjacent sensors was modeled as BSC. However, authors in [17] assumed the received energy emitted by the target at the local sensors was a deterministic value. In this case, the detection performances of the local sensors were similar.

The most common practice of traditional fusion rules, such as CR and Chair-Varshney fusion rules, is to employ all sensors in the ROI to derive a final decision. However, the signal emitted by the target often decays as the distance from the target increases. Sensors far away from the target make little contribution to the final decision at the GFC or are more likely to make a false judgment in the presence of background noise. In this paper, we simply employ sensors around the target to make the final decision.

We propose a new serial topology reconstruction method, where decisions are transmitted from sensors with lower credibility to sensors with higher credibility. Assuming the transmission channels were ideal, we applied a BSF rate of the sensor into the parallel structure and proposed ELRT in [19]. In this paper, we solve the problem when there are failed sensors in the serial structure and propose the corresponding fusion rule over noisy channels which we call serial rule (SR). In order to demonstrate the more stable detection performance of the serial structure, we also extend ELRT to noisy channels and derive the corresponding fusion rule in the same scenario which we call parallel rule (PR).

The remainder of this paper is organized as follows. In Section 2, the BSF rate of the sensor is described. In Section 3, a sensor deployment model is described. In Section 4, a detection system model is described. In Section 5, the fusion rules of the serial and parallel structure are derived. In Section 5, the performance of the proposed fusion rules is provided through simulation. In Section 6, conclusions are drawn.

## 2 BSF rate

One can characterize a lifetime distribution through three functions: reliability function, failure rate function, and mean residual life [20]. The lifetime typically means the time the product can operate regularly before it fails and can be measured in hours, miles, cycles, etc. In our original research work [19], we used failure rate function to characterize the lifetime distribution of electronic components. The failure rate function is shown in Fig. 1, which we call BSF. We can see that the failure rate function has a bathtub shape and can be visually subdivided into three stages: initial failure period, random failure period, and wear-out failure period. The initial failure period starts at zero and decreases noticeably due to early failures caused by design faults or initial implementation problems. The random failure period is relatively flat (approximately constant), which is denoted as the "useful life" phase. The failure is noticeably increasing due to material fatigue or component aging during wear-out failure period [21]. We also gave the modified failure rate function $r(t)$ as follows in [19]

$$r(t) = ab(at)^{b-1} + \left(\frac{a}{b}\right)(at)^{\frac{1}{b}-1} + h_0, \quad t, a, h_0 \geq 0, b > 1 \tag{1}$$

where $a$ and $b$ are related with life data of the products and $h_0$ is a worthy constant adding to the failure rate function.

Thus, sensors in this paper can be classified into four categories

- Normal sensors, sensors that can detect and transmit decision reliably

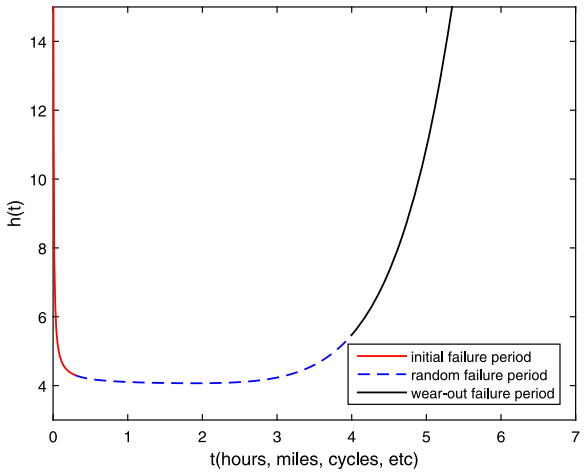


**Fig. 1** BSF rate function according to Eq. (1)

- Partially disable sensors, sensors that are still operable, but have poor detection capability
- Inoperable sensors, sensors which no longer function at all
- Failed sensors, the group of sensors consisting of the combination of the partially disable and the inoperable sensors

Let $N$ denote the initial number of the sensors, $M$ be the number of the sensors excluding the inoperable sensors, $n$ be the number of normal sensors, and $m$ be the number of failed sensors at time $t$, respectively. We can easily get that $n = N - m$. $m$ can be written as

$$m = \text{ceil}\left(\int_0^t r(t)\,dt\right) \tag{2}$$

where ceil $(\cdot)$ denotes the ceiling function.

Irrespective of the inoperable sensors at time $t$, the remaining sensor is either a normal sensor or a partially disable sensor. $R_i = 1$ which represents sensor $s_i$ is a normal sensor, and $R_i = 0$ which represents sensor $s_i$ is a partially disable sensor. The probability that sensor $s_i$ is a partially disable sensor is given as follows

$$\begin{aligned} p_i &= \Pr(R_i = 0) \\ &= \Pr(\textit{sensor } s_i \textit{ is a partially disable sensor}) \\ &= \tfrac{s}{M} \\ &= \tfrac{M-n}{M} \\ &= \tfrac{M-N+m}{M} \quad (0 \le s \le m, 0 < M \le N) \end{aligned} \tag{3}$$

where $s$ is the number of the partially disable sensors at time $t$, it is easy to note that $p_i$ is constant at time $t$ and $\Pr(R_i = 1) = 1 - p_i$. We use $p$ which denotes $\Pr(R_i = 0)$ in the latter sections.

## 3 Sensor deployment model

A sensor deployment example in the presence of failed sensors is shown in Fig. 2. $N$ sensors follow the grid deployment, and a target is deployed randomly in the ROI. The target and different types of sensors are labeled by different symbols. The received signal power emitted by the target $m_i, i = 1, 2, \ldots, N$ of sensor $s_i$ decays as the distance from the target increases. An isotropic attenuation power model adopted in this paper is defined as follows

$$m_i^2 = \frac{P_0 D_0^\gamma}{D_i^\gamma} \tag{4}$$

where $P_0$ is the signal power from the target at a reference distance $D_0$ and $D_i$ represents the Euclidean distance between the target and sensor $s_i$. The signal attenuation exponent $\gamma$ ranges from 2 to 3.

Signal power versus distance from the target is shown in Fig. 3. We can see that target radiation energy decays rapidly as the distance from the target increases. Sensors far away from the target are prone to make wrong decisions influenced by background noise. Authors in [14] establish the precursor-successor relationship among the clusters based on tree topology. The cluster the target located in serves as the root cluster and the other clusters serve as the branch or leaf clusters, in this way, the root cluster can achieve the highest detection performance. Authors in [22] study a binary tree topology, where the sensor nearest the target serves as the root. Authors in [23, 24] think there are several "target spots" in the ROI where the target often appears, then analyze the area centered at the "target spot" and propose a target detection

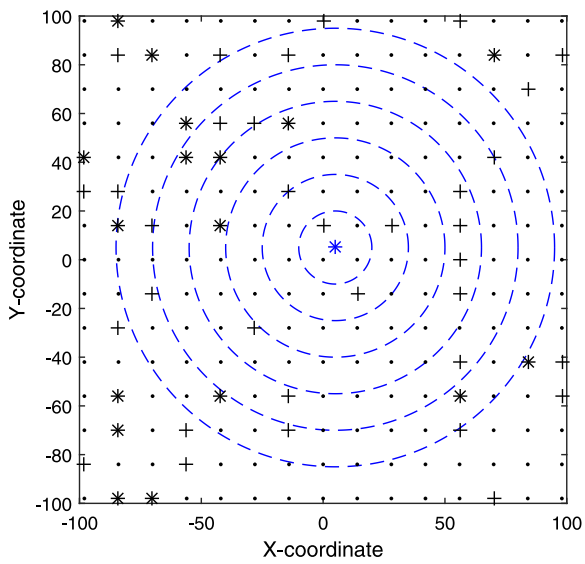


**Fig. 2** A deployment example in the presence of failed sensors. Area of the ROI:$A^2$ ; *black dot*: the normal sensors; *black star*: the inoperable sensors; *black* +: the partially disable sensors; and *blue star*: the target

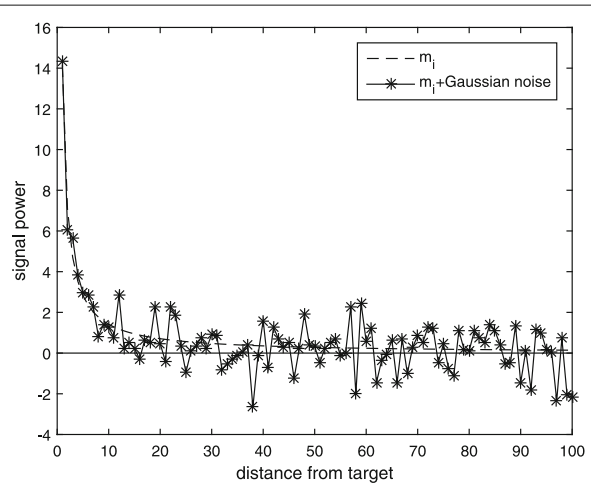


**Fig. 3** Signal power versus distance from target, where $P_0 = 180, D_0 = 1, \gamma = 2$

algorithm based on a probabilistic decision model. So, it is reasonable for us to investigate the area centered at the target in this paper.

The radiation energy of the target can be assumed as a series of concentric circles centered at the target. In this paper, we set the interval between two adjacent circles identical. Sensors lying in the same circular ring possess similar signal-to-noise ratio (SNR) and decision credibility, and the circular ring interval is 10. Due to the fast attenuation of the target radiation energy, we consider the circular area of the radius of 40 centered at the target in this paper. Firstly, sensors in the same circular ring form a serial fragment, then all fragments form the whole serial topology from the outside to the inside. We can see that decisions are transmitted from sensors with lower credibility to sensors with higher credibility in this serial structure, so the final decision at the last sensor of the serial structure possesses the highest credibility.

## 4 System model description

Figure 4 describes the serial detection system model. We leave out the inoperable sensors and form a new serial topology at time $t$. So the serial topology is dynamic. The wireless transmission channel between two adjacent sensors is modeled as BSC with transmission error probability $p_e$. The observation of sensor $s_i$ under each hypothesis is respectively given by

$$\begin{aligned} H_1 &: y_i = m_i + n_i \ ; \ i = 1, \ldots, M^{'} \\ H_0 &: y_i = n_i \qquad ; \ i = 1, \ldots, M^{'} \ \left(M^{'} < N\right) \end{aligned} \tag{5}$$

$H_0$ and $H_1$ denote the absence and the presence of the target to be detected respectively. $M^{'}$ is the number of sensors in the serial topology at time $t$. $y_i$ is the signal received by sensor $s_i$, and $n_i$ is the noise observed by sensor $s_i$. In this paper, we assume that noises at the local sensors are independent identically distributed (i.i.d.) and follow the standard Gaussian distribution, i.e, $n_i \sim N(0,1)$.

In Fig. 4, $v_i$ denotes the decision made by sensor $s_i$, and $u_i$ denotes the bit received by sensor $s_{i+1}$ which may differ from $v_i$. Sensor $s_1$ to $s_{M'}$ cooperatively determine whether the target is present or not in the ROI. Sensor $s_{M'}$ is the fusion center (FC) of the serial structure at time $t$. Because we apply BSF to the serial structure, $s_{M'}$ may be a partially disable sensor. If $s_{M'}$ is a partially disable sensor, the final decision is not reliable. In this paper, we let sensor $s_{M'}$ transmits its observation to the GFC, then the GFC replaces sensor $s_{M'}$ and serves as the FC of the serial structure. In this way, the $M^{'}$th sensor of the serial structure in Fig. 4 is actually the GFC at time $t$.

In Fig. 5, a and b give the local decision-making and transmission process at sensor $s_i$ under the situation of $R_i = 1$ and $R_i = 0$, respectively. Under $H_0$, when $R_i = 1$, sensor $s_i$ makes a correct decision with probability $1 - p_{f,i}$, and an error decision with probability $p_{f,i}$, while when $R_i = 0$, sensor $s_i$ makes a correct decision with probability $1 - p_{f,i}^{'}$, and an error decision with probability $p_{f,i}^{'}$. During the decision transmission process, the bit $u_i$ received by sensor $s_{i+1}$ may differ from the decision $v_i$ made by sensor $s_i$ due to the noisy channel. The situation under $H_1$ is similar to that under $H_0$, except that the detection performance is denoted by $p_{d,i}$ and $p_{d,i}^{'}$. Normally, $p_{d,i}^{'} \le p_{d,i}, p_{f,i} \le p_{f,i}^{'}$.

## 5 SR and PR

### 5.1 SR

Let $p\left(y_i|H_1\right)$ and $p\left(y_i|H_0\right)$ represent the conditional probability density function of the observation $y_i$ at sensor $s_i$ under $H_1$ and $H_0$, respectively. Except that sensor $s_1$ makes the local decision simply according to its observation $y_1$, the other sensors make decision according to their observations and the bit transmitted from the previous sensor. For example, sensor $s_1$ makes a decision $v_1$ according to its observation $y_1$, while sensor $s_2$ makes a decision according to its observation $y_2$ and the bit $u_1$ transmitted from sensor $s_1$, where $u_1$ may be different from $v_1$. For sensor $s_i \left(1 < i \le M^{'} < N\right)$, the decision-making process is similar to sensor $s_2$. The likelihood ratio test at sensor $s_1$ can be expressed as

$$\Lambda_0\left(y_1\right) = \frac{p\left(y_1|H_1\right)}{p\left(y_1|H_0\right)} \underset{H_0}{\overset{H_1}{\gtrless}} \tau \tag{6}$$

Given the local threshold $\tau$ and according to Neyman-Pearson criterion, the detection probability and false

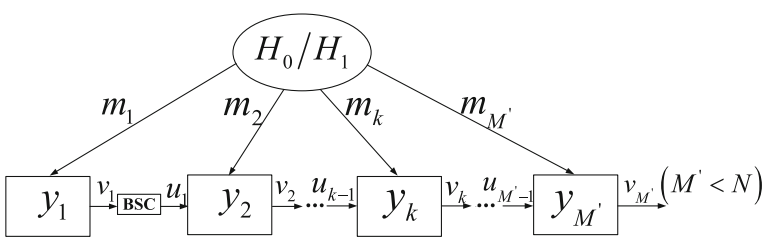


**Fig. 4** Serial detection system model

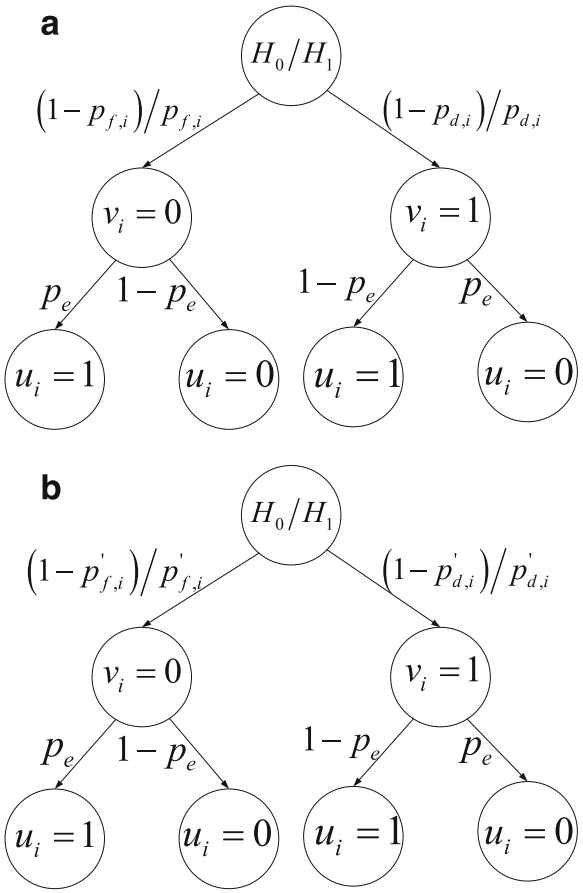


**Fig. 5** Model of serial distributed detection under noisy channel. **a** and **b** describe the situation of $R_i = 1$ and $R_i = 0$, respectively

alarm probability at sensor $s_1$ can be evaluated easily. The likelihood ratio test at sensor $s_i$ $\left(1 < i \leq M^{'} < N\right)$ can be expressed as

$$\Lambda_0\left(y_i\right) = \frac{p\left(y_i, u_{i-1}|H_1\right)}{p\left(y_i, u_{i-1}|H_0\right)} \underset{H_0}{\overset{H_1}{\gtrless}} \tau \tag{7}$$

Because of the independence between $y_i$ and $u_{i-1}$, $\Lambda_0\left(y_i\right)$ can be further expressed as follows

$$\Lambda_0\left(y_i\right) = \frac{p\left(y_i|H_1\right) \cdot p\left(u_{i-1}|H_1\right)}{p\left(y_i|H_0\right) \cdot p\left(u_{i-1}|H_0\right)} \tag{8}$$

Let us discuss $p\left(u_{i-1}|H_1\right)$ firstly. Due to BSC, the received bit $u_{i-1}$ at sensor $s_i$ depends on the decision $v_{i-1}$ made at sensor $s_{i-1}$, thus we can get

$$\begin{aligned} p\left(u_{i-1}|H_1\right) &= \textstyle\sum_{v_{i-1}} p\left(u_{i-1}, v_{i-1}|H_1\right) \\ &= p\left(u_{i-1}, v_{i-1}=1|H_1\right) \\ &\quad + p\left(u_{i-1}, v_{i-1}=0|H_1\right) \\ &= p\left(u_{i-1}|v_{i-1}=1, H_1\right) p\left(v_{i-1}=1|H_1\right) \\ &\quad + p\left(u_{i-1}|v_{i-1}=0, H_1\right) p\left(v_{i-1}=0|H_1\right) \\ &= p\left(u_{i-1}|v_{i-1}=1\right) p\left(v_{i-1}=1|H_1\right) \\ &\quad + p\left(u_{i-1}|v_{i-1}=0\right) p\left(v_{i-1}=0|H_1\right) \end{aligned} \tag{9}$$

In the above equation, we use the Markov property that $u_{i-1}$ is only dependent on $v_{i-1}$. This property will be exploited in the following derivations. Note that the decision $v_{i-1}$ at sensor $s_{i-1}$ depends on whether $s_{i-1}$ is a partially disable sensor or not. Furthermore, we can easily get

$$\begin{aligned} a_{i-1} &= p\left(v_{i-1}=1|H_1\right) \\ &= \textstyle\sum_{R_{i-1}} p\left(v_{i-1}=1, R_{i-1}|H_1\right) \\ &= p\left(v_{i-1}=1, R_{i-1}=1|H_1\right) \\ &\quad + p\left(v_{i-1}=1, R_{i-1}=0|H_1\right) \\ &= p\left(v_{i-1}=1|R_{i-1}=1, H_1\right) p\left(R_{i-1}=1|H_1\right) \\ &\quad + p\left(v_{i-1}=1|R_{i-1}=0, H_1\right) p\left(R_{i-1}=0|H_1\right) \\ &= (1-p)\, p_{d,i-1} + p p^{'}_{d,i-1} \end{aligned} \tag{10}$$

and

$$\begin{aligned} b_{i-1} &= p\left(v_{i-1}=0|H_1\right) \\ &= \textstyle\sum_{R_{i-1}} p\left(v_{i-1}=0, R_{i-1}|H_1\right) \\ &= p\left(v_{i-1}=0, R_{i-1}=1|H_1\right) \\ &\quad + p\left(v_{i-1}=0, R_{i-1}=0|H_1\right) \\ &= p\left(v_{i-1}=0|R_{i-1}=1, H_1\right) p\left(R_{i-1}=1|H_1\right) \\ &\quad + p\left(v_{i-1}=0|R_{i-1}=0, H_1\right) p\left(R_{i-1}=0|H_1\right) \\ &= (1-p)\left(1-p_{d,i-1}\right) + p\left(1-p^{'}_{d,i-1}\right) \end{aligned} \tag{11}$$

when $u_{i-1} = 1$,

$$\begin{aligned} \alpha_{i-1} &= \left(\textstyle\sum_{v_{i-1}} p\left(u_{i-1}, v_{i-1}|H_1\right)\right) | \left(u_{i-1}=1\right) \\ &= (1-p_e)\, a_{i-1} + p_e b_{i-1} \end{aligned} \tag{12}$$

Similarly, when $u_{i-1} = 0$,

$$\begin{aligned} \beta_{i-1} &= \left(\textstyle\sum_{v_{i-1}} p\left(u_{i-1}, v_{i-1}|H_1\right)\right) | \left(u_{i-1}=0\right) \\ &= p_e a_{i-1} + (1-p_e)\, b_{i-1} \end{aligned} \tag{13}$$

So, $p\left(u_{i-1}|H_1\right)$ can be expressed as

$$p\left(u_{i-1}|H_1\right) = \left(\alpha_{i-1}\right)^{u_{i-1}} \cdot \left(\beta_{i-1}\right)^{1-u_{i-1}} \tag{14}$$

Next, let us discuss $p\left(u_{i-1}|H_0\right)$

$$\begin{aligned} p\left(u_{i-1}|H_0\right) &= \textstyle\sum_{v_{i-1}} p\left(u_{i-1}, v_{i-1}|H_0\right) \\ &= p\left(u_{i-1}, v_{i-1}=1|H_0\right) \\ &\quad + p\left(u_{i-1}, v_{i-1}=0|H_0\right) \\ &= p\left(u_{i-1}|v_{i-1}=1, H_0\right) p\left(v_{i-1}=1|H_0\right) \\ &\quad + p\left(u_{i-1}|v_{i-1}=0, H_0\right) p\left(v_{i-1}=0|H_0\right) \\ &= p\left(u_{i-1}|v_{i-1}=1\right) p\left(v_{i-1}=1|H_0\right) \\ &\quad + p\left(u_{i-1}|v_{i-1}=0\right) p\left(v_{i-1}=0|H_0\right) \end{aligned} \tag{15}$$

We can get

$$\begin{aligned} c_{i-1} &= p\left(v_{i-1}=1|H_0\right) \\ &= \textstyle\sum_{R_{i-1}} p\left(v_{i-1}=1,R_{i-1}|H_0\right) \\ &= p\left(v_{i-1}=1,R_{i-1}=1|H_0\right) \\ &\quad +p\left(v_{i-1}=1,R_{i-1}=0|H_0\right) \\ &= p\left(v_{i-1}=1|R_{i-1}=1,H_0\right)p\left(R_{i-1}=1|H_0\right) \\ &\quad +p\left(v_{i-1}=1|R_{i-1}=0,H_0\right)p\left(R_{i-1}=0|H_0\right) \\ &= (1-p)\,p_{f,i-1}+p p^{'}_{f,i-1} \end{aligned} \tag{16}$$

and

$$\begin{aligned} d_{i-1} &= p\left(v_{i-1}=0|H_0\right) \\ &= \textstyle\sum_{R_{i-1}} p\left(v_{i-1}=0,R_{i-1}|H_0\right) \\ &= p\left(v_{i-1}=0,R_{i-1}=1|H_0\right) \\ &\quad +p\left(v_{i-1}=0,R_{i-1}=0|H_0\right) \\ &= p\left(v_{i-1}=0|R_{i-1}=1,H_0\right)p\left(R_{i-1}=1|H_0\right) \\ &\quad +p\left(v_{i-1}=0|R_{i-1}=0,H_0\right)p\left(R_{i-1}=0|H_0\right) \\ &= (1-p)\left(1-p_{f,i-1}\right)+p\left(1-p^{'}_{f,i-1}\right) \end{aligned} \tag{17}$$

when $u_{i-1}=1$,

$$\begin{aligned} \gamma_{i-1} &= \left(\textstyle\sum_{v_{i-1}} p\left(u_{i-1},v_{i-1}|H_0\right)\right)|\left(u_{i-1}=1\right) \\ &= (1-p_e)\,c_{i-1}+p_e d_{i-1} \end{aligned} \tag{18}$$

Similarly, when $u_{i-1}=0$,

$$\begin{aligned} \eta_{i-1} &= \left(\textstyle\sum_{v_{i-1}} p\left(u_{i-1},v_{i-1}|H_0\right)\right)|\left(u_{i-1}=0\right) \\ &= p_e c_{i-1}+(1-p_e)\,d_{i-1} \end{aligned} \tag{19}$$

So, $p\left(u_{i-1}|H_0\right)$ can be expressed as

$$p\left(u_{i-1}|H_0\right)=\left(\gamma_{i-1}\right)^{u_{i-1}}\cdot\left(\eta_{i-1}\right)^{1-u_{i-1}} \tag{20}$$

After a series of derivation, the likelihood ratio test at sensor $s_i$ in Eq. (7) can be formulated as

$$\Lambda_0\left(y_i\right)=\frac{p\left(y_i|H_1\right)}{p\left(y_i|H_0\right)}\left(\frac{\alpha_{i-1}}{\gamma_{i-1}}\right)^{u_{i-1}}\left(\frac{\beta_{i-1}}{\eta_{i-1}}\right)^{1-u_{i-1}}\underset{H_0}{\overset{H_1}{\gtrless}}\tau \tag{21}$$

Now, the decision rule of sensor $s_i$ can be given by

$$\begin{cases} \frac{p(y_i|H_1)}{p(y_i|H_0)}\cdot\frac{\alpha_{i-1}}{\gamma_{i-1}}\underset{H_0}{\overset{H_1}{\gtrless}}\tau, & if\ \ u_{i-1}=1 \\ \frac{p(y_i|H_1)}{p(y_i|H_0)}\cdot\frac{\beta_{i-1}}{\eta_{i-1}}\underset{H_0}{\overset{H_1}{\gtrless}}\tau, & if\ \ u_{i-1}=0 \end{cases} \tag{22}$$

Furthermore, the decision fusion rule in Eq. (22) can be transformed into

$$\Lambda\left(y_i\right)=\frac{p\left(y_i|H_1\right)}{p\left(y_i|H_0\right)}\underset{H_0}{\overset{H_1}{\gtrless}}\begin{cases}\tau_{i,1}, & if\ \ u_{i-1}=1\\ \tau_{i,0}, & if\ \ u_{i-1}=0\end{cases} \tag{23}$$

We should note that $\Lambda\left(y_i\right)$ is another metric we defined and is different from $\Lambda_0\left(y_i\right)$, where

$$\tau_{i,1}=\tau\cdot\tfrac{\gamma_{i-1}}{\alpha_{i-1}},\tau_{i,0}=\tau\cdot\tfrac{\eta_{i-1}}{\beta_{i-1}} \tag{24}$$

The corresponding log-likelihood ratio form of Eq. (23) can be formulated as

$$\Lambda^*\left(y_i\right)=\ln\Lambda\left(y_i\right)\underset{H_0}{\overset{H_1}{\gtrless}}\begin{cases}\tau^{'}_{i,1}=\ln\tau_{i,1}, & if\ \ u_{i-1}=1\\ \tau_{i,0}=\ln\tau_{i,0}, & if\ \ u_{i-1}=0\end{cases} \tag{25}$$

The false alarm probability and the detection probability at sensor $s_i$ are evaluated as follows

$$\begin{aligned} &p_{f,i} \\ &= \Pr\left(\Lambda^*(y_i)\geq\tau^{'}_{i,1}|H_0,u_{i-1}=1\right)\Pr\left(u_{i-1}=1|H_0\right) \\ &\quad+\Pr\left(\Lambda^*(y_i)\geq\tau^{'}_{i,0}|H_0,u_{i-1}=0\right)\Pr\left(u_{i-1}=0|H_0\right) \\ &= \Pr\left(\Lambda^*\left(y_i\right)\geq\tau^{'}_{i,1}|H_0\right)\gamma_{i-1}+\Pr\left(\Lambda^*\left(y_i\right)\geq\tau^{'}_{i,0}|H_0\right)\eta_{i-1} \end{aligned} \tag{26}$$

$$\begin{aligned} &p_{d,i} \\ &= \Pr\left(\Lambda^*(y_i)\geq\tau^{'}_{i,1}|H_1,u_{i-1}=1\right)\Pr\left(u_{i-1}=1|H_1\right) \\ &\quad+\Pr\left(\Lambda^*\left(y_i\right)\geq\tau^{'}_{i,0}|H_1,u_{i-1}=0\right)\Pr\left(u_{i-1}=0|H_1\right) \\ &= \Pr\left(\Lambda^*\left(y_i\right)\geq\tau^{'}_{i,1}|H_1\right)\alpha_{i-1}+\Pr\left(\Lambda^*\left(y_i\right)\geq\tau^{'}_{i,0}|H_1\right)\beta_{i-1} \end{aligned} \tag{27}$$

$p_{f,i}$ and $p_{d,i}$ are recursive equations. If we get the values of $p_{f,1}$ and $p_{d,1}$, $p_{f,M'}$ and $p_{d,M'}$ can be evaluated recursively. Let $P_d$ and $P_f$ represent the global detection probability and false probability, respectively, we note that $P_d=p_{d,M'}$ and $P_f=p_{f,M'}$. Given $\tau$, $p_{f,1}$ and $p_{d,1}$ at sensor $s_1$ can be easily derived according to Eq. (6).

$$p_{f,1}=\int_\tau^\infty\frac{1}{\sqrt{2\pi}}e^{-\frac{x^2}{2}}\,dx=Q\left(\tau\right) \tag{28}$$

$$p_{d,1}=\int_\tau^\infty\frac{1}{\sqrt{2\pi}}e^{-\frac{(x-a_1)^2}{2}}\,dx=Q\left(\tau-\sqrt{\frac{P_0d_0^r}{d_1^r}}\right) \tag{29}$$

where $Q\left(\cdot\right)$ is the complementary distribution function of the standard Gaussian, i.e,

$$Q\left(x\right)=\int_x^\infty\frac{1}{\sqrt{2\pi}}e^{-\frac{z^2}{2}}\,dz \tag{30}$$

### 5.2 PR

To demonstrate the better detection performance of SR, we extend ELRT [19] to noisy channels and propose PR in the same scenario. In the parallel structure, the local sensor $s_i$ makes a local decision $v_{pi}$ $(1\leq i\leq M)$ and transmits it to the GFC in the ROI. We denote $u_{pi}$ as the bit received by the GFC. Due to the BSC, $u_{pi}$ may be different from $v_{pi}$

with transmission error probability $p_e$. Furthermore, we let $\overrightarrow{v_p} = (v_{p1}, v_{p2}, \ldots, v_{pM})$ and $\overrightarrow{u_p} = (u_{p1}, u_{p2}, \ldots, u_{pM})$. Due to the mutual independence among the received bits, the fusion rule at the GFC is given as follows

$$\Lambda_1 = \frac{p\left(\overrightarrow{u_p}|H_1\right)}{p\left(\overrightarrow{u_p}|H_0\right)} = \prod_{i=1}^{M} \frac{p\left(u_{pi}|H_1\right)}{p\left(u_{pi}|H_0\right)} \underset{H_0}{\overset{H_1}{\gtrless}} T \tag{31}$$

According to SR, $\Lambda_1$ can be further represented as

$$\begin{aligned} \Lambda_1 &= \prod_{i=1}^{M} \frac{\sum_{v_{pi},R_i} p\left(u_{pi}, v_{pi}, R_i|H_1\right)}{\sum_{v_{pi},R_i} p\left(u_{pi}, v_{pi}, R_i|H_0\right)} \\ &= \prod_{i=1}^{M} \left(\frac{\alpha_{pi}}{\gamma_{pi}}\right)^{u_{pi}} \left(\frac{\beta_{pi}}{\eta_{pi}}\right)^{1-u_{pi}} \end{aligned} \tag{32}$$

where

$$\begin{cases} \alpha_{pi} = (1-p_e)\, a_{pi} + p_e b_{pi} \\ \beta_{pi} = p_e a_{pi} + (1-p_e)\, b_{pi} \\ \gamma_{pi} = (1-p_e)\, c_{pi} + p_e d_{pi} \\ \eta_{pi} = p_e c_{pi} + (1-p_e)\, d_{pi} \end{cases}$$

$$\begin{cases} a_{pi} = (1-p)\, p_{p,di} + p p^{'}_{p,di} \\ b_{pi} = (1-p)\left(1-p_{p,di}\right) + p\left(1-p^{'}_{p,di}\right) \\ c_{pi} = (1-p)\, p_{p,fi} + p p^{'}_{p,fi} \\ d_{pi} = (1-p)\left(1-p_{p,fi}\right) + p\left(1-p^{'}_{p,fi}\right) \end{cases}$$

where $T$ denotes the detection threshold at the GFC, $p_e$ and $p$ are given in the previous section. $p_{p,di}$ and $p^{'}_{p,di}$ denote the local detection probability when sensor $s_i$ is a normal sensor and a partially disable sensor, respectively. Similarly, $p_{p,fi}$ and $p^{'}_{p,fi}$ denote the local false probability. Given the local threshold, according to Neyman-Pearson criterion, we can get the local detection probability and false probability easily. The log-likelihood ratio form is given as follows

$$\Lambda_1^{'} = \ln \Lambda_1 = \sum_{i=1}^{M} \left(u_{pi} \ln\left(\frac{\alpha_{pi}\eta_{pi}}{\gamma_{pi}\beta_{pi}}\right) + \ln\left(\frac{\beta_{pi}}{\eta_{pi}}\right)\right) \tag{33}$$

The final fusion rule at the GFC is as follows

$$\Lambda_1^{'} \underset{H_0}{\overset{H_1}{\gtrless}} T_1 \tag{34}$$

where $T_1 = \ln T$. We use $P_{pd}$ and $P_{pf}$ to represent the global detection probability and false probability of the parallel structure respectively. $P_{pd}$ and $P_{pf}$ can be evaluated as

$$\begin{aligned} P_{pd} &= \Pr\left(\Lambda_1^{'} > T_1|H_1\right) \\ P_{pf} &= \Pr\left(\Lambda_1^{'} > T_1|H_0\right) \end{aligned} \tag{35}$$

## 6 Performance analysis

We use the Matlab simulator to evaluate the performance of the proposed fusion rules in this paper, and $10^4$ Monte Carlo runs are used in each simulation. The objective is to demonstrate that serial structure has more stable detection performance than the parallel structure in the presence of a vast number of failed sensors. In [19], we studied the parallel distributed detection applying BSF rate of the sensor over ideal channels and proposed ELRT rule. Simulations demonstrated that ELRT outperformed Chair-Varshney rule in the presence of failed sensors. In this paper, we apply BSF to the serial structure over noisy channels and also extend ELRT to noisy channels, because sensors far away from the target make little contributions to the final decision at the GFC and are more likely to make wrong decisions in the presence of background noise. Thus, we consider sensors within the circular area centered at the target in this paper, the deployment in the presence of failed sensors is presented in Fig. 2. The fusion rules of the serial and parallel are given in the previous sections.

In Fig. 6, according to Eq. (2), the number of failed sensors including the partially disable sensors and the inoperable sensors is plotted as a function of $t$(hours, miles, cycles, etc) and the corresponding parameters are given at the bottom. We can see that the number of failed sensors during the initial failure period is negligible, such as $t = 0.5$. The number increases slowly at the low time, while the number grows noticeably after time 5. The curve of the number of failed sensors over time also reflects the feature of BSF.

We leave out the inoperable sensors at each time, the partially disable sensors are selected from the remaining sensors randomly. In Fig. 7, a and b show the receiver

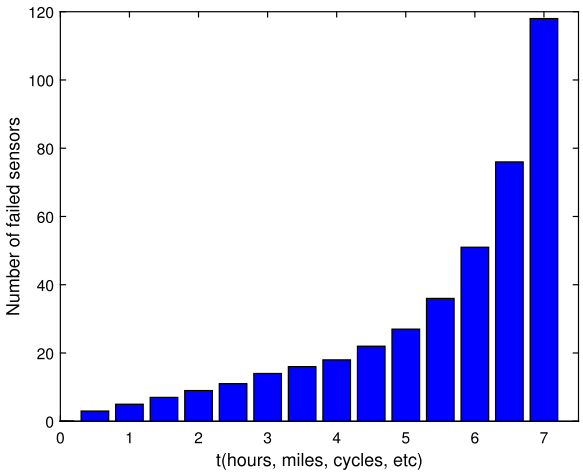


**Fig. 6** The number of failed sensors obtained by Eq. (2) at a different time: $a = 0.25$, $b = 8$, and $h_0 = 4$

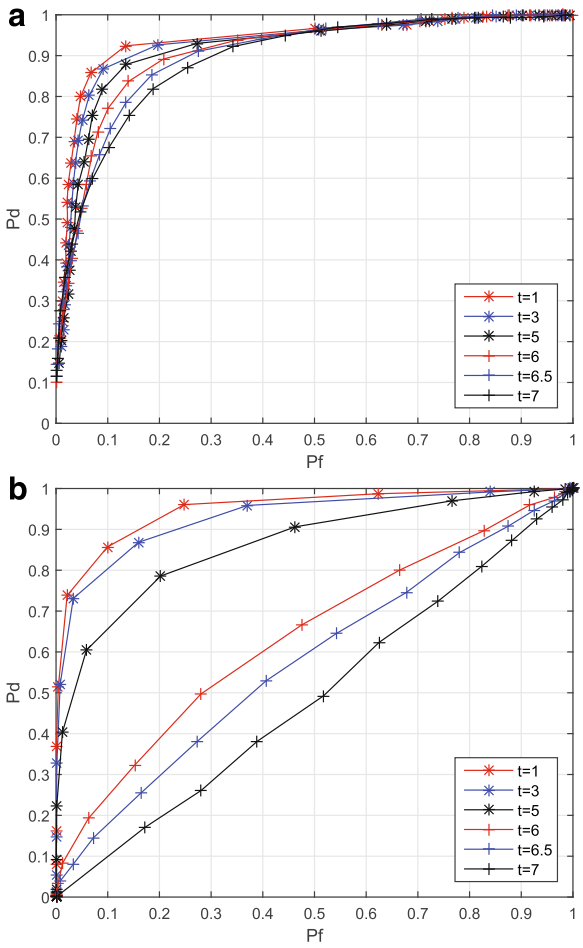


**Fig. 7** The ROC curses of SR and PR at a different time: $\gamma = 2$, $A = 200$ m, $D_0 = 1$ m, $N = 220$, $P_0 = 180$, $\frac{N-M}{m} = \frac{1}{3}$, $p_{d,i}^{'} = \frac{p_{d,i}}{5}$, $p_{f,i}^{'} = 0.5$, $a = 0.25$, $b = 8$, and $h_0 = 4$. **a**, **b** correspond to the ROC curses of SR and PR, respectively

operating characteristic (ROC) curves for SR and PR, respectively. The simulation parameters for these two rules are set to be identical and given at the bottom. We use $t = 1, t = 3, t = 5, t = 6, t = 6.5$, and $t = 7$ to conduct the experiment and choose $p_{d,i}^{'} = p_{d,i}/5$ and $p_{f,i}^{'} = 0.5$ for the partially disable sensor due to their poor performance. In Fig. 7a, we see that the performance of SR decreases slightly all the time. In Fig. 7b, we observe that the performance of PR decreases slowly before time 5 and noticeably after time 5. For PR, sensors in the parallel structure make local decisions and transmit the decisions to the GFC directly. At the low time, a small number of failed sensors have a negative but not big effect on the system performance. Meanwhile, at the high time, a large number of failed sensors have a major negative effect on the system performance. For SR, each sensor in the serial structure makes a decision according to the bit transmitted from the previous sensor and the state (partially disable or normal) of the previous sensor, and due to this cooperative detection, SR has more stable detection performance even in the presence of a large number of failed sensors at high time. We should note that BSF influences the detection performances of both serial and parallel structures.

The above analysis demonstrates the effectiveness of SR. In order to investigate the impact of SNR on the detection performance of SR, Fig. 8 shows the global detection probability $P_d$ versus SNR over time. SNR is defined as the ratio of source energy to the standard deviation of noise, namely $\mathrm{SNR} = 10\log\left(\frac{S}{N}\right)$, where $S = P_0, N = 1$ in this paper. We can see that higher SNR leads to higher global detection probability. Comparing the curves at a different time, it is easy to note that when SNR is fixed, detection probability at a lower time is superior to higher time, and this is in accordance with the results of ROC.

## 7 Conclusions

This paper investigates distributed decision fusion of serial structure in the presence of failed sensors over noisy channels. Previous literature focus on serial structure usually assumes the signal received by the local sensor is identical. While in this paper we construct a serial topology based on isotropic attenuation power model, the local decision in this topology is transmitted from sensors with lower credibility to sensors with higher credibility. We also derive the corresponding fusion rule. For comparison, we extend ELRT to noisy channels in the same scenario. Simulations show that serial is more robust than parallel in the presence of a large number of failed sensor over noisy channels. The deployment we considered in this paper is relatively ideal, we will study different deployment in the future.

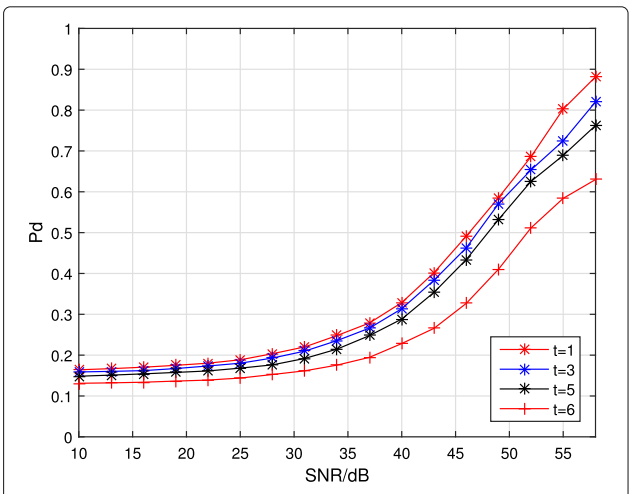


**Fig. 8** Global detection probability of SR versus SNR

**Acknowledgements**
This work was supported in part by the Overseas Academic Training Funds, University of Electronic Science and Technology of China (OATF, UESTC) (Grant No. 201506075013), and the Program for Science and Technology Support in Sichuan Province (Grant nos. 2014GZ0100 and 2016GZ0088).

**Authors' contributions**
JL conceived of and designed the research. JL and ZL performed the experiments and analyzed the result. JL and ZL wrote the paper. Both authors read and approved the final manuscript.

**Competing interests**
The authors declare that they have no competing interests.

## Publisher's Note



Received: 20 January 2016 Accepted: 30 June 2017
Published online: 14 July 2017

**References**

1. Z Chair, PK Varshney, Optimal data fusion in multiple sensor detection systems. IEEE Trans. Aerosp. Electron. Syst. **22**(1), 98–101 (1986)
2. IY Hoballah, PK Varshney, Distributed Bayesian signal detection. IEEE Trans. Inf. Theory. **35**(5), 995-1000 (1989)
3. T-L Chin, YH Hu, Optimal Detector Based on Data Fusion for Wireless Sensor Networks, Global Telecommunications Conference (GLOBECOM 2011). IEEE, Kathmandu, Nepal. **6613**(1), 1–5 (2011)
4. R Niu, PK Varshney, Q Cheng, Distributed detection in a large wireless sensor network. Inf. Fusion. **7**(4), 380–394 (2006)
5. R Niu, PK Varshney, Distributed Detection and Fusion in a Large Wireless Sensor Network of Random Size. EURASIP J. Wirel. Commun. Netw. **2005**(4), 462–472 (2005)
6. Decentralized binary detection with noisy communication links. IEEE Trans. Aerosp. Electron. Syst. **42**(4), 1554–1563 (2006)
7. K Eritmen, M Keskinoz, Distributed decision fusion over fading channels in hierarchical wireless sensor networks. Wirel. Netw. **20**(5), 987–1002 (2014)
8. R Niu, B Chen, PK Varshney, Fusion of decisions transmitted over Rayleigh fading channels in wireless sensor networks. IEEE Trans. Signal Process. **54**(3), 1018–1027 (2006)
9. Y Xia, F Wang, W-S Deng, The decision fusion in the wireless network with possible transmission errors. Inf. Sci. **199**(15), 193–203 (2012)
10. Y Lin, B Chen, PK Varshney, Decision fusion rules in multi-hop wireless sensor networks. IEEE Trans. Aerosp. Electron. Syst. **41**(2), 475–488 (2005)
11. AM Aziz, A new multiple decisions fusion rule for targets detection in multiple sensors distributed detection systems with data fusion. Inf. Fusion. **18**(1), 175–186 (2014)
12. J-Y Wu, C-W Wu, T-Y Wang, et al., Channel-aware decision fusion with unknown local sensor detection probability. IEEE Trans. Signal Process. **58**(3), 1457–1463 (2010)
13. D Ciuonzo, PS Rossi, Decision fusion with unknown sensor detection probability. IEEE Signal Process. Lett. **21**(2), 208–212 (2014)
14. H Huang, L Chen, X Cao, et al., Weight-based clustering decision fusion algorithm for distributed target detection in wireless sensor networks. Int. J. Distrib. Sensor Netw. **2013**, 1–9 (2013)
15. G Ferrari, M Martalo, R Pagliari, Decentralized detection in clustered sensor networks. IEEE Trans. Aerosp. Electron. Syst. **47**(2), 959–973 (2011)
16. Q Tian, EJ Coyle, Optimal distributed detection in clustered wireless sensor networks. IEEE Trans. Signal Process. **55**(7), 3892–3904 (2007)
17. L Yin, Y Wang, D-W Yue, *Serial Distributed Detection Performance Analysis in Wireless Sensor Networks Under Noisy Channel, Wireless Communications, Networking and Mobile Computing*. (IEEE, Beijing, 2009), pp. 3092–3095
18. M Lucchi, M Chiani, *Distributed Detection of Local Phenomena with Wireless Sensor Networks, 2010 IEEE International Conference on Communications (ICC 2010)*. (IEEE, Cape Town), pp. 1–6
19. J Luo, T Li, Bathtub-shaped failure rate of sensors for distributed detection and fusion. Math. Probl. Eng. **2014**, 1–8 (2014)
20. CD Lai, M Xie, DNP Murthy, in *Advances in Reliability*. Chapter 3. Bathtubshaped failure rate life distributions, vol. 20 of Handbook of Statistics. (2001), pp. 69–104
21. M Bebbington, C-D Lai, R Zitikis, Useful periods for lifetime distributions with bathtub shaped hazard rate functions. IEEE Transactions on Reliability. **55**, 245–251 (2006)
22. J Ni, J Mei, *A Fusion Algorithm for Target Detection in Distributed Sensor Networks. Computational Intelligence and Communication Networks (CICN)*. (IEEE, Bhopal, 2014), pp. 349–353
23. T Wang, Z Peng, J Liang, et al., *Detecting Targets Based on a Realistic Detection and Decision Model in Wireless Sensor Networks. International Conference on Wireless Algorithms, Systems, and Applications WASA*. (Springer, 2015), pp. 836–844
24. T Wang, Z Peng, C Wang, et al., Extracting Target Detection Knowledge Based on Spatiotemporal Information in Wireless Sensor Networks. Int. J. Distrib. Sensor Netw. **2016**, 1–11 (2016)